Three Dimensional Simulation of Jet Formation in Collapsing Condensates

Weizhu Bao[1], D. Jaksch[2], and P.A. Markowich[3]
[1] *Department of Computational Science, National University of Singapore, Singapore 117543.*
[2] *Clarendon Laboratory, Department of Physics, University of Oxford, Oxford, United Kingdom.*
[3] *Institute of Mathematics, University of Vienna Boltzmanngasse 9, A-1090 Vienna, Austria.*
(Dated: February 2, 2008)

We numerically study the behavior of collapsing and exploding condensates using the parameters of the experiments by E.A. Donley *et al.* [Nature, **412**, 295, (2001)]. Our studies are based on a full three-dimensional numerical solution of the Gross-Pitaevskii equation (GPE) including three body loss. We determine the three body loss rate from the number of remnant condensate atoms and collapse times and obtain only one possible value which fits with the experimental results. We then study the formation of jet atoms by interrupting the collapse and find very good agreement with the experiment. Furthermore we investigate the sensitivity of the jets to the initial conditions. According to our analysis the dynamics of the burst atoms is not described by the GPE with three body loss incorporated.

PACS numbers: 03.75.Fi, 42.50.-p, 42.50.Ct

arXiv:cond-mat/0307344v1 15 Jul 2003

I. INTRODUCTION

Most of the single particle properties of Bose-Einstein condensates (BEC) in dilute weakly interacting gases are well described by the Gross-Pitaevskii equation (GPE) (for reviews see [1, 2, 3]). The GPE is well suited for investigating static as well as dynamic properties of a BEC and also allows to investigate the stability of BECs with attractive interactions in a trapping potential. Inelastic processes which only become important for large particle densities are usually accounted for by adding cubic and quintic damping terms to the GPE which are believed to properly describe two- and three-particle loss, respectively.

In early experiments on BEC with attractive interactions [4] the scattering length was fixed and limited the size of these condensates to a number $N_{\rm cr}$ [5] which for typical experimental parameters was on the order of $N_{\rm cr} \approx 1000$. In these experiments a collapse of the condensate was induced stochastically while growing the BEC out of a thermal cloud of atoms. In contrast, more recent experiments by Donley *et al.* [6] allowed to deterministically induce collapses of the condensate which revealed a dramatic behavior for a ^{85}Rb BEC. In these experiments the sign of the scattering length is changed from positive (repulsive interaction) to negative (attractive interaction) values by an external magnetic field. This sudden change in the sign of the interaction leads to a series of collapses and explosions, a dynamical behavior which provides a very good opportunity for testing the applicability of the GPE.

In particular the nature of the atoms emitted in a burst during the collapse of the condensate is not very well understood at present [7]. While some numerical studies [8, 9] indicate that these atoms are produced coherently and can be described by the GPE, other numerical [10] and analytical approaches [11, 12, 13, 14, 15] conclude that these atoms are not described by the GPE alone.

The numerical studies arrive at different conclusions mostly due to the choice of the three particle loss rate near the Feshbach resonance. The work of Saito and Ueda [8] predicts a series of collapses and explosions during the experiment and correctly reproduces the burst atoms by choosing a three particle loss rate that is smaller than the one used by Adhikari [10] where one big collapse determines most of the behavior of the condensate and the burst atoms are not reproduced correctly. Varying the three particle loss rate with the scattering length [9] to match the burst energies allows to get good quantitative agreement with the experimental data.

In the analytical approach by Duine and Stoof [15] elastic binary collisions in the BEC are suggested to cause the bursts and in [13] the dynamics of collective excitations driven by the collapsing condensate are investigated analytically and found to explain the overall features of collapsing and exploding condensates. The effect of a molecular state close to threshold near a Feshbach resonance on the interaction between the atoms is explored in [11, 12, 14]. In fact, such novel interaction mechanisms arising close to Feshbach resonances which are not contained in the GPE could yield the relatively large burst energies seen in the experiment [12].

In this paper we study numerically the full three dimensional GPE with attractive interactions including three particle loss. We first choose the three-body loss rate K_3^0 to match the observed remnant condensate particle numbers and collapse times. We find only one single value for K_3^0 which fits the experimental data and subsequently use this value in our numerics. Then we investigate the time evolution of the collapsing condensate. We find jets of atoms whose particle number and sensitivity to initial conditions is in quantitative agreement with the experiment by Donley et al. [6]. The results of our comparison can be seen in Fig. 1 where we plot the number of jet atoms as a function of the time $\tau_{\rm evolve}$ at which the collapse of the condensate is interrupted. Also, the shape and energies of the jets agree with the experiment. We do not, however, find burst atoms with energies as

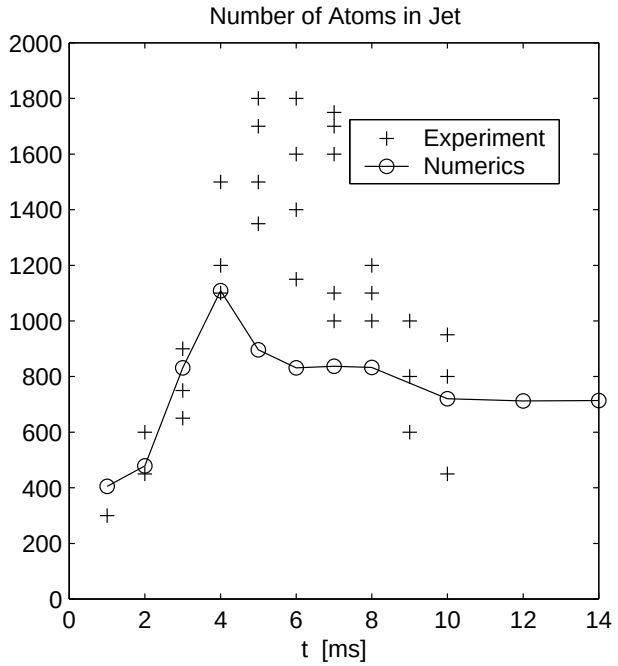

FIG. 1: Number of atoms in the jets as a function of time $\tau_{\rm evolve}$ [ms] (labelled as t) for $a_{\rm init} = 7a_0$, $N_0 = 16000$ and $a_{\rm collapse} = -30a_0$. '+ +': Experimental data from [6]. '–o–': Numerical results for parameters equivalent to those used in the experiment.

measured in the experiment and thus conclude that they are not described by the physics contained in the GPE alone.

For our numerical studies we use the time-splitting sine-spectral method (TSSP) recently introduced by Bao *et al.* for solving the damped GPE [16, 17]. This method is explicit, unconditionally stable, time transversal invariant, and of spectral accuracy in space and second order accuracy in time. It thus yields reliable results even in the case of having sharply peaked wave functions during the collapse.

The paper is organized as follows: In Sec. II we will introduce the GPE including loss terms and present the numerical method we use to solve it. Then, in Sec. III we first adjust the three particle loss rate to match the experimental results for the number of remnant particles and the collapse time. This is followed by a detailed comparison of numerical and experimental results on the jet atoms and bursts of atoms. Finally in Sec. IV we draw some conclusions.

II. MODEL AND NUMERICAL METHOD

In this section we will first introduce the GPE used for describing the dynamics of a BEC with varying interaction strength. Then we briefly present the numerical method for solving this three dimensional nonlinear partial differential equation.

A. Model

We consider a one component BEC with varying scattering length that is described by the GPE including a damping term that accounts for inelastic interactions

$$i\hbar\frac{\partial\psi(\mathbf{x},t)}{\partial t} = \left(-\frac{\hbar^2\nabla^2}{2m} + V(\mathbf{x}) + U(t)|\psi|^2 - i\,\frac{g(|\psi|^2)}{2}\right)\psi, \tag{1}$$

for times $t > 0$ with the initial condition

$$\psi(\mathbf{x}, t=0) = \psi_0(\mathbf{x}). \tag{2}$$

Here $\psi(\mathbf{x},t)$ is the macroscopic wave function of the condensate, and $\mathbf{x} = (x,y,z)^T$ is the spatial coordinate. We assume the trapping potential to be harmonic $V(\mathbf{x}) = m\left(\omega_x^2x^2 + \omega_y^2y^2 + \omega_z^2z^2\right)/2$ with ω_x, ω_y, ω_z the trapping frequencies in x, y, and z direction respectively, and m the mass of the atoms.

The macroscopic wave function at time $t = 0$, i.e. the initial data ψ_0, is normalized

$$\int_{\mathbf{R}^3} |\psi(\mathbf{x},0)|^2\, d^3\mathbf{x} = \int_{\mathbf{R}^3} |\psi_0(\mathbf{x})|^2\, d^3\mathbf{x} = N_0, \tag{3}$$

where N_0 is the total number of condensate particles at time $t = 0$. The two-body interaction between the atoms is given by $U(t) = 4\pi\hbar^2a_s(t)/m$ with $a_s(t)$ the s-wave scattering length. In the experiment the time dependence of $a_s(t)$ (cf. Fig. 2) [6] is realized by changing the magnitude of an external magnetic field near a Feshbach resonance of the ^{85}Rb atoms.

In the case of a positive scattering length a_s the GPE (1) with $g \equiv 0$ has a stable ground state solution $\psi_{\rm gs}(\mathbf{x})$ while if the sign of $a_s(t)$ is changed from positive to negative the GPE becomes focusing and does not have a stable ground state solution anymore, i.e., the condensate may collapse. As in the experiment we will start our simulations at positive scattering lengths a_s and for most of the calculations assume the BEC initially to be in its ground state [18, 19] corresponding to the initial condition Eq. (2) with $\psi_0(\mathbf{x}) = \psi_{\rm gs}(\mathbf{x})$.

Loss from the condensate is described by the term $g(\rho) = \hbar\left(K_2(t)\rho + K_3(t)\rho^2\right)$ where $K_2(t)$ is due to two-body dipolar loss and $K_3(t)$ accounts for the three-body recombination inelastic processes. We assume the effects of $K_2(t)$ to be negligible and set $K_3(t)$ equal to K_3^0 when $a_s(t) = a_{\rm collapse}$, and 0 otherwise [6, 8, 15]. Furthermore we assume K_3^0 to be proportional to $a_{\rm collapse}^2$ [8, 10]. Under this assumption we choose K_3^0 to match the number of remnant atoms in the condensate after the collapse and the collapse times observed in the experiments. We also compare its value with experimental data in [23].

B. Dimensionless GPE

In our numerical computations, we simulate and present numerical results based on the following dimensionless GPE. We introduce $\tilde{t} = \omega_z t$, $\tilde{\mathbf{x}} = \mathbf{x}/l_0$,

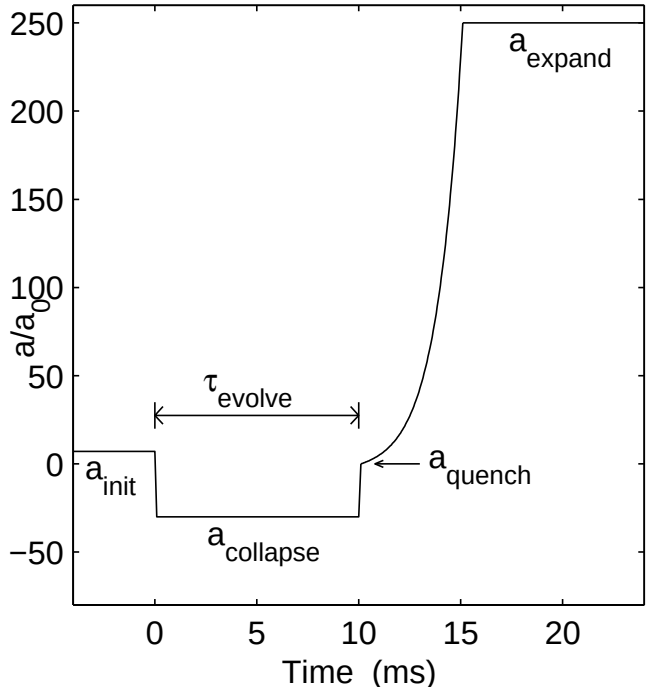

FIG. 2: Example of a time dependence of the scattering length a_s during the experiment [6]. A condensate with ground state wave function $\psi_0(\mathbf{x})$ is prepared at $a_s = a_{\rm init}$. Then the collapse is induced by going to a negative scattering length for a time $\tau_{\rm evolve}$ and finally the time evolution of the remaining particles is studied at large positive values of a_s.

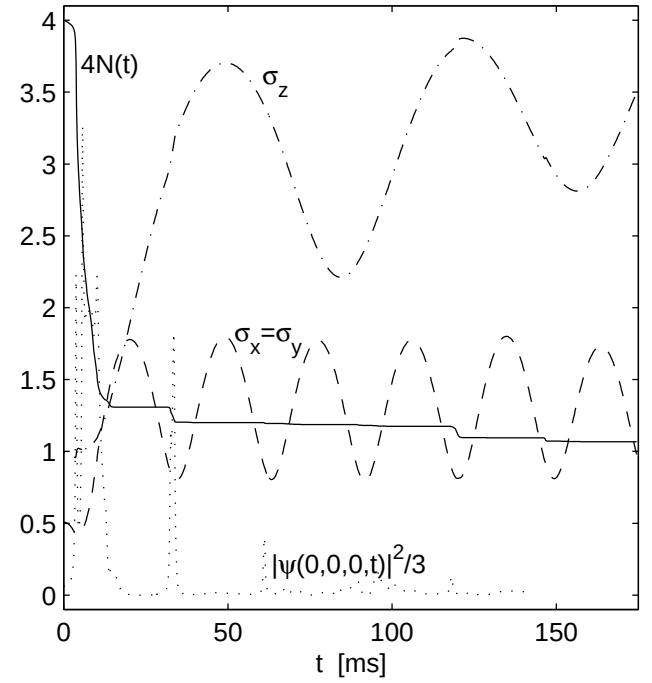

FIG. 3: Normalization, condensate widths and central density $|\psi(0,0,0,t)|^2$ as functions of time $\tau_{\rm evolve}$ [ms] (labelled as t) for $a_{\rm init} = 7a_0$, $a_{\rm collapse} = -30a_0$ and $N_0 = 16000$.

$\tilde{\psi}(\tilde{\mathbf{x}},\tilde{t}) = l_0^{3/2}\psi(\mathbf{x},t)/\sqrt{N_0}$, $\tilde{\psi}_0(\tilde{\mathbf{x}}) = l_0^{3/2}\psi_0(\mathbf{x})/\sqrt{N_0}$, with $l_0 = \sqrt{\hbar/m\omega_z}$ the size of the harmonic oscillator ground state. the dimensionless time and length units respectively. Substituting into Eq. (1), multiplying both sides by $l_0^{3/2}/\hbar\omega_z\sqrt{N_0}$, and removing all $\tilde{}$, we obtain the following dimensionless GPE

$$i\,\frac{\partial\psi(\mathbf{x},t)}{\partial t} = \left(-\frac{\nabla^2}{2} + V(\mathbf{x}) + \beta(t)|\psi|^2 - i\,\frac{g(|\psi|^2)}{2}\right)\psi, \tag{4}$$

with the initial condition

$$\psi(\mathbf{x},t=0) = \psi_0(\mathbf{x}); \tag{5}$$

where $\beta(t) = 4\pi a_s(t)N_0/l_0$, $g(\rho) = \delta_1(t)\beta_c N_0\rho + \delta_2(t)\beta_c^2 N_0^2\rho^2$, $\delta_1(t)$ and $\delta_2(t)$ equal to δ_1^0 and δ_2^0 respectively when $a_s(t) = a_{\rm collapse}$, and 0 otherwise, $V(\mathbf{x}) = \frac{1}{2}\left(\gamma_x^2x^2 + \gamma_y^2y^2 + z^2\right)$ with $\gamma_x = \omega_x/\omega_z$ and $\gamma_y = \omega_y/\omega_z$, $\beta_c = 4\pi|a_{\rm collapse}|/l_0$, $\delta_1^0 = K_2^0/\left(l_0^3\omega_z\beta_c\right)$, $\delta_2^0 = K_3^0/\left(l_0^6\omega_z\beta_c^2\right)$. For $a_s(t) = a_{\rm collapse} < 0$ we therefore have $\beta(t) = -\beta_c N_0$. The macroscopic wave function ψ in the dimensionless GPE (4) is now normalized to 1 at time $t = 0$, i.e.,

$$\int_{\mathbf{R}^3} |\psi(\mathbf{x},0)|^2\,d^3\mathbf{x} = \int_{\mathbf{R}^3} |\psi_0(\mathbf{x})|^2\,d^3\mathbf{x} = 1. \tag{6}$$

We assume that δ_1^0 and δ_2^0 are independent of N_0 and $a_{\rm collapse}$ [8, 10].

The fraction of particles $N_\Omega(t)$ in a volume Ω is given by

$$N_\Omega(t) = \int_\Omega |\psi(\mathbf{x},t)|^2\,d^3\mathbf{x}, \tag{7}$$

and therefore the number of condensate particles in a volume Ω is $N_0\ N_\Omega(t)$. Due to the loss term $g(|\psi|^2)$ the total number of particles $N_{\rm total}(t) = N_0\ N(t) = N_0\ N_{\mathbf{R}^3}(t)$ is time dependent, decaying as

$$\dot{N}_{\rm total}(t) = -N_0\int_{\mathbf{R}^3} g(|\psi(\mathbf{x},t)|^2)|\psi(\mathbf{x},t)|^2\,d^3\mathbf{x} \le 0. \tag{8}$$

We do not further care for the particles lost from the BEC by inelastic collisions and concentrate on the dynamics of the remaining condensate particles. However, particles incoherently lost from the condensate might still be observed in an experiment. We also introduce the mean width of the condensate in directions x, y, z (cf. Fig. 3) which is computed from the wave function as

$$\sigma_\alpha^2(t) = \int_{\mathbf{R}^3} \alpha^2\,|\psi(\mathbf{x},t)|^2\,d^3\mathbf{x}/N(t), \quad \alpha = x,y,z. \tag{9}$$

C. Numerical method

We use the time splitting sine-spectral method (TSSP) which is described in detail in [16, 17] for solving

the damped GPE. This method for numerically solving Eq. (4) is based on a time-splitting, where at every time step one solves

$$i\,\frac{\partial\psi(\mathbf{x},t)}{\partial t} = -\frac{\nabla^2}{2}\psi, \tag{10}$$

followed by evolving

$$i\,\frac{\partial\psi(\mathbf{x},t)}{\partial t} = \left(V(\mathbf{x}) + \beta(t)|\psi|^2 - i\,\frac{g(|\psi|^2)}{2}\right)\psi. \tag{11}$$

The linear Schrödinger equation without external potential Eq. (10) can be discretized in space by the sine-spectral method and then sovled in time *exactly* when homogeneous Dirichlet boundary conditions are applied [16]. For each fixed $\mathbf{x}$, the ordinary differential equation (ODE) Eq. (11) can be integrated *exactly*, too [16]. In fact, the TSSP for the GPE combines the advantages of the spectral method which yields spectral order accuracy in space and can generate simple and explicit numerical formulae for partial differential equations (PDEs) with constant coefficients when a proper orthogonal basis is chosen, and the split-step method which can decouple nonlinear PDEs, e.g. the GPE, into linear PDEs with constant coefficients and a nonlinear ODE which can usually be solved analytically. The merit of the TSSP for solving the GPE is that it is explicit, unconditionally stable, time reversible and time transverse invariant when the GPE is, of spectral order accuracy in space and of second order accuracy in time, conserves the total number of particles for the GPE (1) without damping, i.e. for $g \equiv 0$, and exactly reproduces the decay rate of the total number of particles for the GPE (1) with a linear damping term, i.e. $g \equiv \alpha_0 > 0$.

It is well known that the three-dimensional cubic nonlinear Schrödinger equation (NLS) (i.e. GPE without external potential) with sufficiently large attractive two-body interaction leads to finite-time collapse of the spatial condensate density [20, 21, 22], i.e. $|\psi|^2$ becomes a delta distribution for some finite value of time, and afterwards the solution ceases to exist. This collapse mechanism is halted by the three-body recombination term, which starts to kick in when the density becomes too large locally and then acts to instantaneously reduce the density in an explosion-like process [20, 21]. We remark that the mathematical analysis of the GPE with loss terms Eq. (4) is not well developed yet, a systematic study has just begun right now.

III. RESULTS

Before presenting the results of our numerical studies we adjust the three particle loss rate by fitting the numerical results to the experimental data for the remnant number of condensate atoms and the time of the collapse. Then we study the formation of jet atoms and study their sensitivity to initial conditions. Finally we investigate bursts of atoms and present results of the simulations that do not agree with the experiment.

A. Experimental parameters and three particle loss rate

To determine the three particle loss rate we use the experimental results for a collapsing condensate of ^{85}Rb particles measured in [6] where a condensate of ^{85}Rb, with a particle mass $m = 1.406 \times 10^{-25}$kg, trapping frequencies $\omega_x = \omega_y = 2\pi \times 17.5$/s, and $\omega_z = 2\pi \times 6.8$/s, i.e. a cylindrically symmetric geometry were used. In the experiment at time $t = 0$ a BEC with $N_{\rm total}(0) = N_0 = N_0\ N(0) = 16000$ atoms and a scattering length of $a_s(0) = 7a_0$ (where a_0 is the Bohr radius) is prepared. Afterwards, by changing the external magnetic field, the scattering length is linearly ramped down to $a_s = a_{\rm collapse} = -30a_0$ (which corresponds to $\beta_c = 4.7717 \times 10^{-3}$) in time $t = 0.1$ms and held there for a time $\tau_{\rm evolve}$ as schematically shown in Fig. 2. This process leads to a strongly attractive and unstable condensate which undergoes a sequence of collapses and explosions before finally a remnant condensate with particle number $N^0_{\rm remnant}$ is left. The remnant condensate is then measured at a positive scattering length (cf. Fig. 2).

We use the same time dependence for the scattering length a_s in our numerics to find the quintic damping term δ_2^0. Assuming cubic damping to be negligible we set $\delta_1^0 = 0$ and fit the parameter of the dominant quintic damping term δ_2^0 according to the experimental results for $a_{\rm collapse} = -30a_0$, i.e. the number of remnant atoms in the condensate after the collapse and the collapse times observed in the experiments. We simulate the experiment and adjust the three particle loss rate to numerically obtain a number of remnant atoms that agrees with the experiment. Fig. 4 shows the number of atoms in the condensate for different values of δ_2^0. From this figure, we find a unique solution for the loss rate δ_2^0 given by $\delta_2^0 = 1.3 \times 10^{-3}$ which corresponds to a three particle loss rate of $K_3^0 = \delta_2^0 l_0^6 \omega_z \beta_c^2 = 6.756 \times 10^{-27}$ [cm^6/s]. This value for three particle loss is in agreement with the measured values shown in Fig. 2c of Ref. [23] and we use it for all of the following computations. We will check agreement of the numerics with the experimental results for the remnant condensate particle number and the collapse times.

1. Remnant condensate particles

In Fig. 5 we show the comparison between the experimental and our numerical results for the number of remnant condensate particles $N_{\rm remnant}$ as a function of the time $\tau_{\rm evolve}$. The results are in quantitative agreement as can be seen from Fig. 5. We fit our results for $N_{\rm remnant}$ to a smooth function of the form $N_{\rm remnant}(\tau_{\rm evolve}) = N^0_{\rm remnant} + (N_0 - N^0_{\rm remnant}) \cdot \exp((t_{\rm collapse} - \tau_{\rm evolve})/t_{\rm decay})$

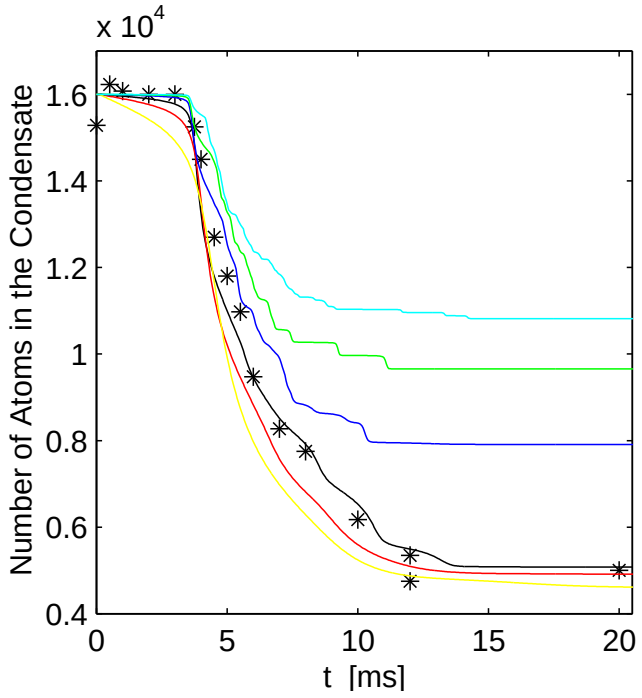

FIG. 4: Number of remaining atoms after collapsing a ^{85}Rb condensate of $N_0 = 16000$ atoms with different values for the three-body loss rate δ_2^0. Collapse is achieved by ramping the scattering length linearly from $a_{\rm init} = 7a_0$ to $a_{\rm collapse} = -30a_0$ in 0.1 [ms] as a function of time $\tau_{\rm evolve}$ [ms] (labelled as t). The '*' are taken from the experiment [6]. Curves are displayed in the order of decreasing $N^0_{\rm remnant}$ for: Cyan: $\delta_2^0 = 0.00005$ (i.e. $K_3^0 = 2.598 \times 10^{-28}$ [cm^6/s]); Green: $\delta_2^0 = 0.00016$ (i.e. $K_3^0 = 8.315 \times 10^{-28}$ [cm^6/s]); Blue: $\delta_2^0 = 0.0004$ (i.e. $K_3^0 = 2.079 \times 10^{-27}$ [cm^6/s]); Black: $\delta_2^0 = 0.0013$ (i.e. $K_3^0 = 6.756 \times 10^{-27}$ [cm^6/s]); Red: $\delta_2^0 = 0.003$ (i.e. $K_3^0 = 1.559 \times 10^{-26}$ [cm^6/s]); Yellow: $\delta_2^0 = 0.008$ (i.e. $K_3^0 = 4.157 \times 10^{-26}$ [cm^6/s]).

where $N^0_{\rm remnant}$ gives the number of condensate particles for $\tau_{\rm evolve} \to \infty$, $t_{\rm collapse}$ gives the time at which the condensate starts to collapse, and $t_{\rm decay}$ is the decay time constant that determines the loss of particles during the collapse. The values found in the experiment were $t_{\rm collapse} = 3.8, 8.6$ [ms] and $N^0_{\rm remnant} = 5000, 7000$ for $a_{\rm collapse} = -30a_0, -6.7a_0$, respectively which is in agreement with our numerical simulation where we get $t_{\rm collapse} = 3.6, 9.35$ [ms] and $N^0_{\rm remnant} = 5075, 6970$ for $a_{\rm collapse} = -30a_0, -6.7a_0$, respectively. We find decay times $t_{\rm decay} = 2.8, 2.8$ [ms] (cf. Fig. 5) for $a_{\rm collapse} = -30a_0, -6.7a_0$, respectively, which also agrees with the experiment. Furthermore, from our numerical simulation for $a_{\rm collapse} = -250a_0$ we find $N^0_{\rm remnant} \approx 1660$, $t_{\rm decay} = 1.2$ [ms] and $t_{\rm collapse} = 1.1$ [ms].

2. *Collapse time*

Using the same value for δ_2^0 we can also confirm the experimentally observed change in the time at which the condensate collapses as a function of the density of the initial condensate. In Fig. 6 we show the number of condensate particles for $N_0 = 6000$, $a_{\rm collapse} = -15a_0$ and two different initial condensate densities with $a_{\rm init} = 0$ and $a_{\rm init} = 89a_0$. We find numerically $t_{\rm collapse} = 5.7,\ 16.2$ [ms] for $a_{\rm init} = 0,\ 89a_0$ respectively, which is in excellent agreement with the experiment [6].

3. *Nature of the collapse*

Our simulations reveal a series of collapses and explosions similarly to the experiment. In Fig. 3 we plot the particle density in the center of the trap as well as the widths of the condensate wave function in the different directions x, y, z. The fraction of condensate particle number $N(t)$ is also shown. The first collapse is marked by a sharp increase in the particle density in the center of the trap. During this first collapse a large amount of the particles is lost from the condensate. For the parameters chosen in Fig. 3 subsequent collapses are by far less important than the first one as they have only a minor effect on the particle numbers. Also the peak density of these collapses is much smaller than for the first collapse and the widths of the condensate wave function are hardly affected. The times at which subsequent collapses happen are determined by the stiffer oscillation frequencies in the harmonic trap (see Fig. 3), i.e. as soon as those particles emitted during a collapse return to the z-axis the particle density in the center increases and the next collapse happens.

The surface plots in Fig. 7 give a more detailed view of the evolution of the condensate density during the collapse. First the condensate contracts in the center of the trap and the particle density increases (Fig. 7a,b). During the first collapse a number of sharp peaks forms in the vicinity of the trap center (Fig. 7c,d) which subsequently, towards the end of the first collapse, spread out due to their kinetic energy (Fig. 7e,f). As we will show later these peaks are not of sufficient kinetic energy to produce the bursts of atoms seen in the experiment but interference effects between them [8] lead to the formation of the jets.

Finally we note that our three dimensional simulations allow this degree of agreement with the experiment only for the three particle loss rate δ_2^0 chosen above. Simulations using smaller [8] or larger [10] three particle loss rates do not yield numerical results that agree with the experimental data.

B. Jet formation

Next we are interested in the formation of jet atoms as observed in the experiment and thus simulate the following sequence for $a_s(t)$ (cf. Fig. 2): at $t = 0$ the scattering length a_s is ramped linearly from $a_{\rm init}$ to $a_{\rm collapse}$ in 0.1 [ms], then kept constant for a time $\tau_{\rm evolve}$ (during this

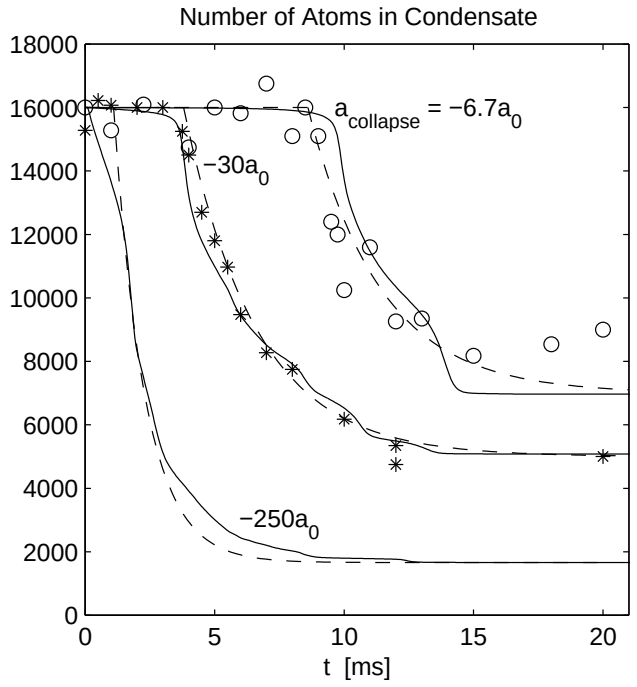

FIG. 5: Number of remaining atoms after collapsing a ^{85}Rb condensate of $N_0 = 16000$ atoms. Collapse is achieved by ramping the scattering length linearly from $a_{\rm init} = 7a_0$ to $a_{\rm collapse} = -6.7a_0, -30a_0$ and $-250a_0$ in 0.1 [ms] as a function of time $\tau_{\rm evolve}$ [ms] (labelled as t). The '*' and 'o' are taken from the experiment [6], the solid curves are our numerical solutions and the dashed curves are fitted to the experimental points: $N_{\rm total}(t) = N_{\rm remnant}(\tau_{\rm evolve}) = N^0_{\rm remnant} + (N_0 - N^0_{\rm remnant})\cdot\exp((t_{\rm collapse} - \tau_{\rm evolve})/t_{\rm decay})$ with $N^0_{\rm remnant} =$ 7000, 5000, 1660; $t_{\rm collapse} = 8.6,\ 3.8,\ 1.1$ [ms] and $t_{\rm decay} = 2.8,\ 2.8,\ 1.2$ [ms] for $a_{\rm collapse} = -6.7a_0,\ -30a_0,\ -250a_0$, respectively.

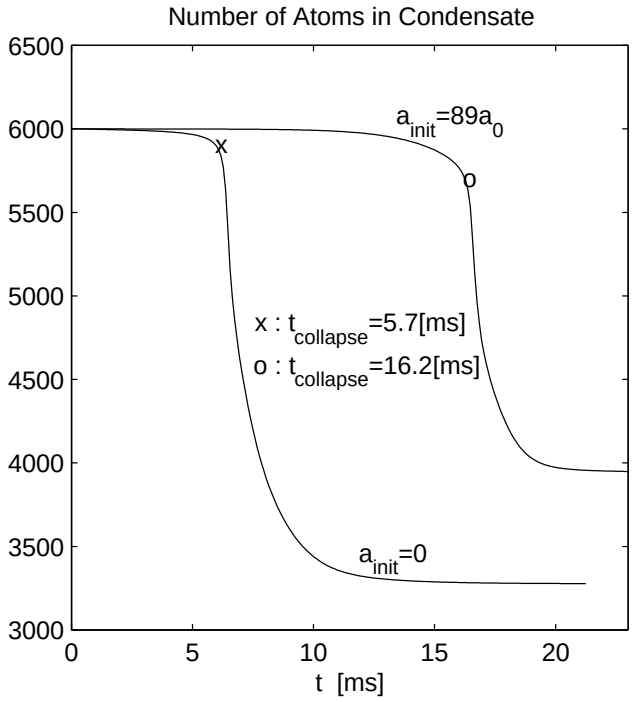

FIG. 6: Number of remnant atoms in the ^{85}Rb condensate for $N_0 = 6000$ after ramping the scattering length linearly from $a_{\rm init} = 0$ and $a_{\rm init} = 89a_0$ at $t = 0$ to $a_{\rm collapse} = -15a_0$ at $t = 0.1$ [ms] as a function of time $\tau_{\rm evolve}$ [ms] (labelled as t).

time period we apply the damping term in our numerics). Then the collapse is interrupted by switching a_s linearly back from $a_{\rm collapse}$ to $a_{\rm quench} = 0$ in 0.1 [ms], followed by changing a_s exponentially from $a_{\rm quench}$ to $a_{\rm expand}$ in 5 [ms]. Then it is kept constant at $a_s = a_{\rm expand}$. The resulting condensate density is shown in Fig. 8 where we can see the emergence of jet atoms and their dynamics.

For $\tau_{\rm evolve} < t_{\rm collapse}$, i.e. before the condensate starts to collapse the outer region of the condensate is already affected by the negative scattering length and begins to expel some particles. As soon as the collapse has started this effect becomes more vigorous and condensate particles are ejected from the core of the condensate dominantly in the xy plane forming jets. As the collapse continues, i.e. $\tau_{\rm evolve}$ increases, the number of particles in the jet first becomes larger and then towards the end of the first collapse (cf. also Fig. 5 and Fig. 3 for the duration of the first collapse) decreases again. Finally, when the collapse is allowed to complete no jets can be seen anymore. The numerical results for the number of jet atoms as a function of $\tau_{\rm evolve}$ can be seen in Fig. 1. We count the number of atoms in the jets from the atom density $|\psi|^2$ over a jet domain defined by $[-5,-0.75]^2 \times [-0.75, 0.75] \cup [0.75, 5]^2 \times [-0.75, 0.75]$, and acquire the image 5.2 [ms] after applying $a_{\rm quench}$) [24]. These numerical results agree with the experimental data very well and also the jet pictures in Fig. 8 which give an impression on the shape of the jets agree well with those observed experimentally.

A large variance in the number of jet particles was found in the experiment. A possible reason for this could be that the initial condensate was not prepared exactly in the ground state. Then, if the jets are formed by interferences of particles emitted from different point like peaks in the atomic density [8] as shown in Fig. 7 slight deviations in the initial condition from the ground state wave function may have a big influence on the numbers of particles in the jets. We have tested this assumption by introducing a small offsets of the initial condensate wave function from the center of the trap and indeed found large variations in the jet particle number. A typical example is given in Fig. 9 where an asymmetric jet of atoms can be seen. For small times $\tau_{\rm evolve}$ the behavior of the condensate is very similar to the case of a centered BEC shown in Fig. 8. This is in accordance with the small variance in the particle number for $\tau_{\rm evolve} < 4$ms observed experimentally. For larger times $\tau_{\rm evolve}$ the behavior of the condensate with an initial offset is significantly different from the centered case; an asymmetric jet is formed in Fig. 9 and we find large changes in the number of jet

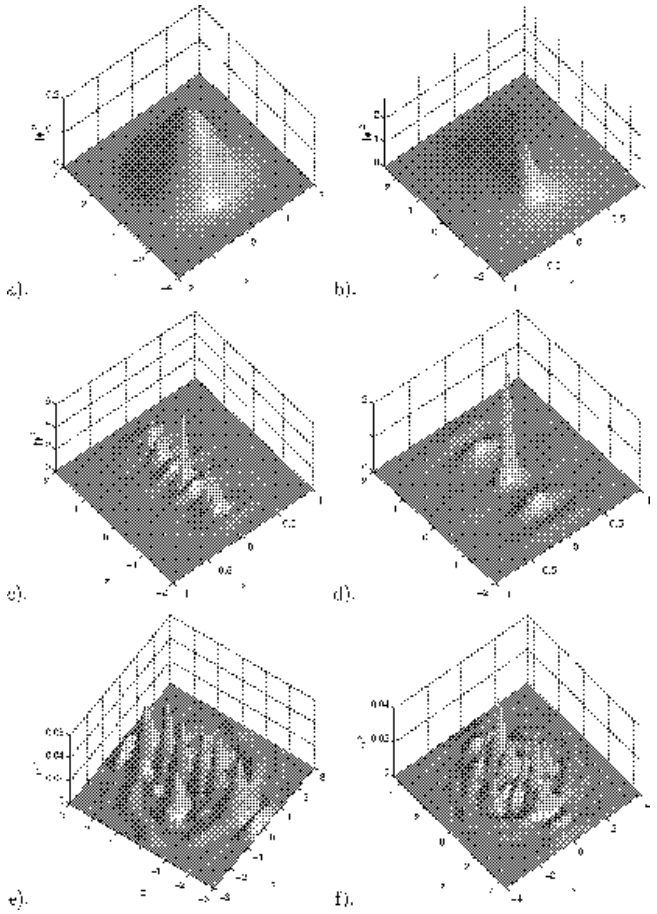

FIG. 7: Surface plot of the density function $|\psi|^2$ in BEC with $a_{\text{init}} = 7a_0$, $a_{\text{collapse}} = -30a_0$ and $N_0 = 16000$. At times τ_{evolve} (in [ms]) a). 0, b). 3.51, c). 10.53, d). 14.04, e). 17.55, f). 21.06.

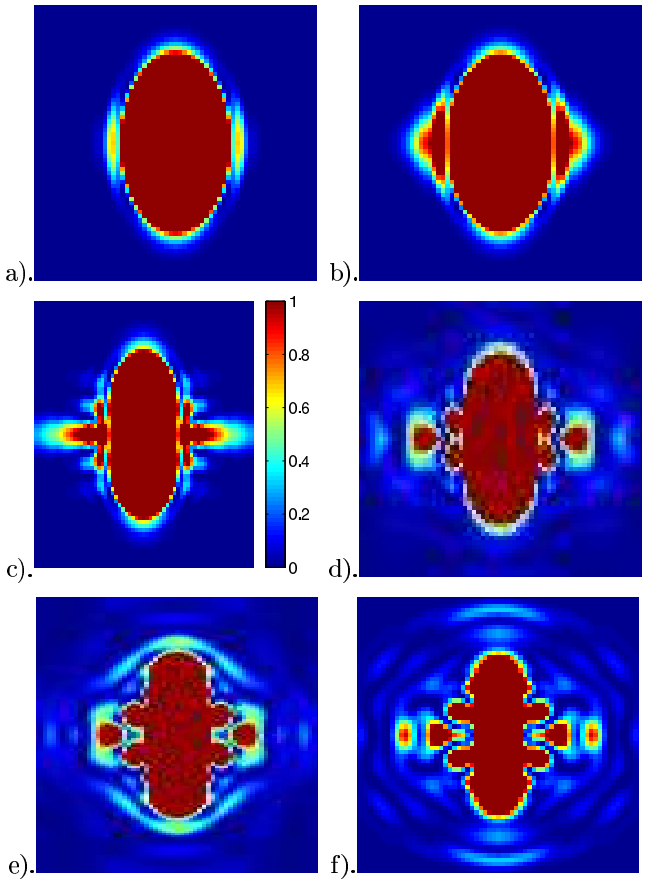

FIG. 8: Jet images (i.e. image of $|\psi(x,0,z,t)|^2$) for a series of τ_{evolve} values for $a_{\text{init}} = 7a_0$, $N_0 = 16000$ and $a_{\text{collapse}} = -30a_0$. The evolution times τ_{evolve} were 2, 3, 4, 6, 8 and 10 [ms] (from a) to f)). $a_{\text{quench}} = 0$ and $a_{\text{expand}} = 250a_0$. The time from the application of a_{quench} until the acquisition of the images was equal to 5.2 [ms].

particles for small offsets in qualitative agreement with the experimentally observed values. The offset chosen in Fig. 9 corresponds to an initial potential energy of the condensate of $E_p \approx 0.47\hbar\omega_z$ and thus to a temperature of $T \approx 0.15$nK. Therefore it seems plausible that even small temperatures - although they might not lead to an offset of the condensate as chosen in our numerical example - and/or uncertainties in the initial wave function can influence the jet formation and lead to the large variance seen in the experiment.

C. Bursts of atoms

Finally we also want to study the bursts of atoms observed in the experiments [6]. The bursts are particles that are emitted from the condensate at relatively high energies when the collapse is allowed to complete. For finding the burst particles we compute $\phi_z(z,t)$ and $\phi_{xy}(x,y,t)$ as the axially and radially averaged density cross-sections, respectively, as follows:

$$\phi_z(z,t) = \int_{-\infty}^{\infty}\int_{-\infty}^{\infty} |\psi(x,y,z,t)|^2 \, dxdy, \qquad (12)$$

$$\phi_{xy}(x,y,t) = \int_{-\infty}^{\infty} |\psi(x,y,z,t)|^2 \, dz. \qquad (13)$$

Choosing a core domain $\Omega_0 = [-b_x,b_x]\times[-b_y,b_y]\times[-b_z,b_z]$ and domains $\Omega_z = \mathbf{R}\setminus[-b_z,b_z]$, $\Omega_{xy} = \mathbf{R}^2\setminus[-b_x,b_x]\times[-b_y,b_y]$ [24], we calculate the expectation value of the axial and radial potential energy per particle in the region Ω_z and Ω_{xy} respectively

$$E_{\text{Axial}}(t) = \frac{\int_{\Omega_z}\frac{1}{2}z^2\phi_z(z,t)\,dz}{\int_{\Omega_z}\phi_z(z,t)\,dz},$$

$$E_{\text{Radial}}(t) = \frac{\int_{\Omega_{xy}}\frac{1}{2}\left(\gamma_x^2x^2+\gamma_y^2y^2\right)\phi_{xy}(x,y,t)\,dxdy}{\int_{\Omega_{xy}}\phi_{xy}(x,y,t)\,dxdy},$$

and the number of atoms inside the core of the conden-

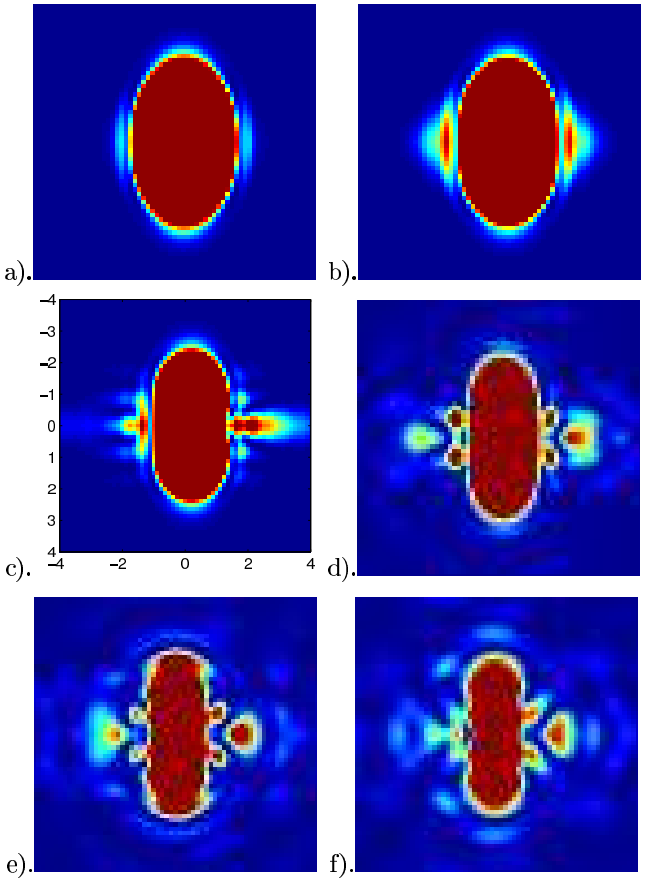

FIG. 9: Jet images for time $\tau_{\rm evolve}$ at 2, 3, 4, 6, 8 and 10 [ms] (from a) to f)) when we shift the center of the initial data from the origin to $(0.375, 0, 0)$. All other parameters as in Fig. 1.

sate

$$N_{\rm in}(t) = N_0 \int_{\Omega_0} |\psi|^2 \, d\mathbf{x}, \qquad N_{\rm out}(t) = N_{\rm total}(t) - N_{\rm in}(t),$$

where $b_x = b_y = 1.5$ and $b_z = 2.5$ from our simulation for $a_{\rm init} = 0$. Figure 10 shows these potential energies and the number of atoms in the condensate for $N_0 = 6000$ and $a_{\rm collapse} = -30a_0$. We find qualitative agreement between numerics and experiment in the number of burst atoms and the revival time, i.e. the time when the radial energy $E_{\rm Axial}(t)$ has a minimum. However, the energy at which the atoms are emitted are far too small in our simulation and rather correspond to the energies at which the jet atoms are formed. Within our model of the three dimensional GPE with three particle loss we were only able to find particles emitted from the condensate at energies comparable to those observed experimentally if we decreased the three particle loss rate as done in the simulations of [8]. Decreasing the three particle loss rate leads to a more pronounced peak in the wave function and higher particle densities during the collapse and thus to higher kinetic energies of the particles leaving the condensate. However, such small values of the three

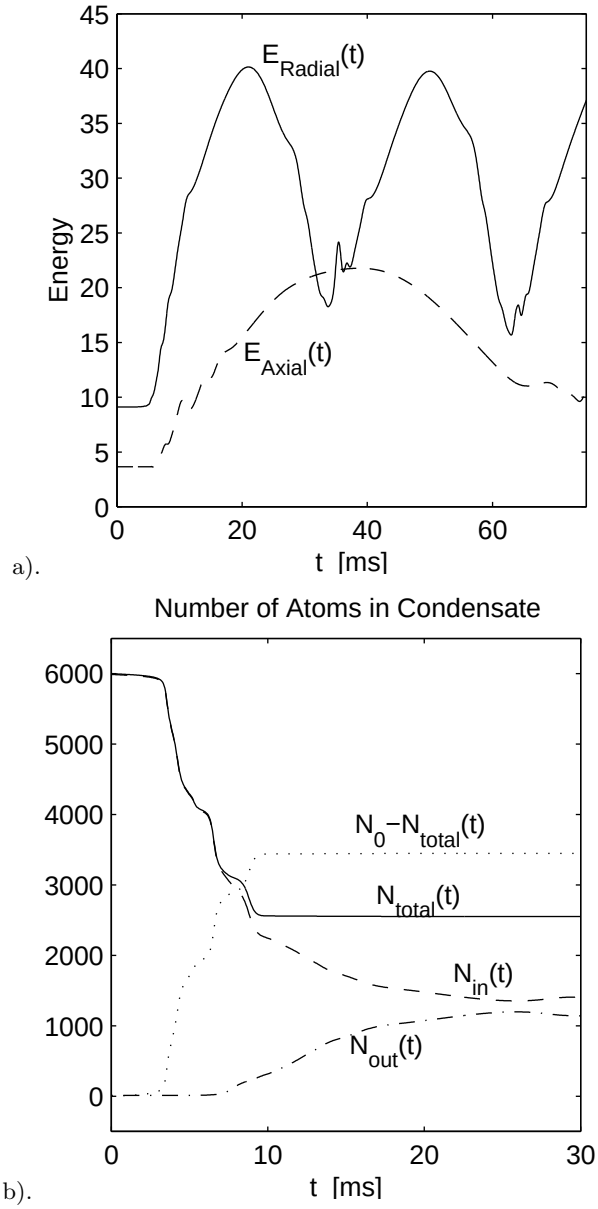

FIG. 10: a) Radial and axial potential energy per particle outside the core of the condensate as functions of time $\tau_{\rm evolve}$ [ms] (labelled as r) and b) number of atoms inside and outside of the core of the condensate. We have chosen $a_{\rm init} = 0$, $N_0 = 6000$, and $a_{\rm collapse} = -30a_0$.

particle loss rate are ruled out by the above considerations in Sec. III A. Therefore we conclude that the three dimensional GPE with three particle loss is not able to describe all the features observed in the experiment [6] correctly and some additional physical mechanisms like those investigated in [11, 12, 14, 15] need to be taken into account.

IV. CONCLUSIONS

In conclusion we have shown that the GPE describes the physics of collapsing and exploding condensates apart from the energies of the burst atoms for the chosen three particle loss rate K_3^0. We also found that no value for K_3^0 reproduces all the aspects of this experiment correctly. We obtained excellent agreement for the number of remnant atoms and the collapse times. Also the jets of atoms are well reproduced by the GPE and we found that small variations in the initial condition for the wave function yield big changes in the number of jet atoms. The large fluctuations in the number of jet atoms observed in the experiment could thus be due to uncertain initial conditions.

Acknowledgments

W.B. acknowledges support by the National University of Singapore. P.A.M. acknowledges support from the EU-funded network 'HYKE', and from his WITTGENSTEIN-AWARD, funded by the Austrian National Science Fund FWF. D.J acknowledges support from the WITTGENSTEIN-AWARD of P. Zoller. This research was supported in part by the International Erwin Schrödinger Institute in Vienna.

[1] E. Cornell, Very cold indeed: The nanokelvin physics of Bose-Einstein condensation, J. Res. Natl. Inst. Stan. **101**, 419 (1996).
[2] F. Dalfovo, S. Giorgini, L.P. Pitaevskii and S. Stringari, Rev. Mod. Phys. 71, 1999, 463.
[3] J.R. Anglin and W. Ketterle, Nature (London) **416**, 211 (2002).
[4] C.C. Bradley, C.A. Sackett, J.J. Tollet, and R. Hulet, Phys. Rev. Lett. **75**, 1687 (1995).
[5] Y. Kagan, A.E. Muryshev and G.V. Shlyapnikov, Phys. Rev. Lett. **81**, 1998, 933.
[6] E.A. Donley, N.R. Claussen, S.L. Cornish, J.L. Roberts, E.A. Cornell and C.E. Wieman, Dynamics of collapsing and exploding Bose-Einstein condensates, Nature, 412, 295-299, 2001.
[7] C. M. Savage, N. P. Robins, and J. J. Hope, Phys. Rev. A **67**, 014304 (2003).
[8] H. Saito and M. Ueda, Phys. Rev. Lett. **86**, 1406, 2001; H. Saito and M. Ueda, Phys. Rev. A **65**, 033624 (2002).
[9] L. Santos and G. V. Shlyapnikov, Phys. Rev. A **66**, 011602 (2002).
[10] S. K. Adhikari, Phys. Rev. A **66**, 013611 (2002).
[11] M. Mackie, K.-A. Suominen, and J. Javanainen, Phys. Rev. Lett. **89**, 180403 (2002).
[12] J. N. Milstein, C. Menotti, M. J. Holland, cond-mat/0303211.
[13] E. Calzetta, B. L. Hu, cond-mat/0207289.
[14] T. Koehler, T. Gasenzer, K. Burnett, cond-mat/0209100.
[15] R. A. Duine and H. T. C. Stoof, Phys. Rev. Lett. **86**, 2204 (2001).
[16] W. Bao and D. Jaksch, An explicit unconditionally stable numerical method for solving damped nonlinear Schrödinger equations with a focusing nonlinearity, SIAM J. Numer. Anal., to appear; arXiv: math.NA/0303158, 2003.
[17] W. Bao, D. Jaksch and P.A. Markowich, Numerical solution of the Gross-Pitaevskii equation for Bose-Einstein condensation, J. Comput. Phys. **187**, 318 (2003).
[18] W. Bao and Q. Du, Computing the ground state solution of Bose-Einstein condensates by a normalized gradient flow, arXiv: cond-mat/0303241, 2003.
[19] W. Bao and W. Tang, Ground state solution of trapped interacting Bose-Einstein condensate by by directly minimizing the energy functional, J. Comput. Phys. **187**, 230 (2003).
[20] G. Fibich, Self-focusing in the damped nonlinear Schrödinger equation, SIAM J. Appl. Math., 61(2001), pp. 1680-1705.
[21] G. Fibich and G. Papanicolaou, Self-focusing in the perturbed and unperturbed nonlinear Schrödinger equation in critical dimension, SIAM J. Appl. Math., 60(2000), pp. 183-240.
[22] C. Sulem and P.L. Sulem, The Nonlinear Schrödinger Equation: Self-focusing and Wave Collapse, Springer, New York, 1999.
[23] J.L. Roberts, N.R. Claussen, S.L. Cornish and C.E. Wieman, Magnetic field dependence of ultracold inelastic collisions near a Feshbach resonance, arXiv: physics/0003027, 2000.
[24] We use domains defined in cartesian coordinates rather than adhering to the cylindrical symmetry of the problem as this corresponds more closely to the experimental way of measuring the corresponding properties.